Anal. Chem. **2010,** *82,* 5810–5814

Multiplex Single Nucleotide Polymorphism Genotyping Utilizing Ligase Detection Reaction Coupled Surface Enhanced Raman Spectroscopy

Adam J. Lowe,*,† Yun Suk Huh,‡,|| Aaron D. Strickland,§ David Erickson,‡ and Carl A. Batt§

Graduate Field of Microbiology, Sibley School of Mechanical and Aerospace Engineering and Department of Food Science, Cornell University, Ithaca, New York 14853, and Division of Materials Science, Korea Basic Science Institute, Daejeon 305-333, Korea

Single nucleotide polymorphisms (SNPs) are one of the key diagnostic markers for genetic disease, cancer progression, and pharmcogenomics. The ligase detection reaction (LDR) is an excellent method to identify SNPs, combining low detection limits and high specificity. We present the first multiplex LDR-surface enhanced Raman spectroscopy (SERS) SNP genotyping scheme. The platform has the advantage in that the diagnostic peaks of Raman are more distinct than fluorescence, and in theory, a clinically significant number of markers can be multiplexed in a single sample using different SERS reporters. Here we report LDR-SERS multiplex SNP genotyping of K-Ras oncogene alleles at 10 pM detection levels, optimization of DNA labeling as well as Raman conditions, and the linear correlation of diagnostic peak intensity to SNP target concentration in heterozygous samples. Genomic DNA from typed cells lines was obtained and scored for the K-Ras genotype. These advances are significant as we have further developed our new SNP genotyping platform and have demonstrated the ability to correlate genotype ratios directly to diagnostic Raman peak signal intensity.

SNPs are clinically useful for disease diagnosis and the selection of the appropriate therapies.[1−3] The ability to genotype multiple SNPs in limited clinical samples is important due to their potential for heterogeneous distribution. For example, oncogenic K-Ras alleles have been detected at G12V, G12A, G13D, and Q61R.[4] The K-Ras genotype from a patient's tumor is highly informative, as tumors with different genotypes respond differently to treatment regiments.[5−7] Many methodologies have been previously developed for SNP genotyping. Strategies include primer elongation via PCR, enzymatic cleavage, hybridization, and LDR (oligonucelotide ligation), with most of them relying on a fluorescent spectra or mass spectrometry for signal output.[8] Fluorescence is limited as a multiplex reporter due to spectral overlap. Mass spectrometry is able to deconvolute more complex mixtures since different mass tags can be used,[9,10] but the equipment is cumbersome and difficult to integrate into a diagnostic device with a small footprint.

We have recently developed a technology that utilizes SERS to circumvent the spectral overlap of fluorescence spectroscopy while retaining sensitivity and accuracy of LDR for SNP detection.[11] Detection schemes utilizing SERS are advantageous over fluorescence as Raman peaks are approximately 1 nm[12] full width half-maximum (fwhm) while fluorescent labels can be 100 times larger fwhm.[13] In addition to our LDR-SERS platform, Raman spectroscopy has been utilized for DNA identification and SNP detection using hybridization platforms[14,15] as well as PCR based systems.[16] Importantly, multiplex identification systems have been developed utilizing SERS technologies that require no additional data processing other than simple peak recognition.[16−18]

* Corresponding author. E-mail: ajl248@cornell.edu. Fax: 607-255-8741. Phone: 607-255-7902.

† Graduate Field of Microbiology, Cornell University.

‡ Sibley School of Mechanical and Aerospace Engineering, Cornell University.

|| Korea Basic Science Institute.

§ Department of Food Science, Cornell University.

(1) Ching, A.; Caldwell, K. S.; Jung, M.; Dolan, M.; Smith, O. S.; Tingey, S.; Morgante, M.; Rafalski, A. J. *BMC Genet.* **2002**, *3*, 19.

(2) Mehta, A. M.; Jordanova, E. S.; Corver, W. E.; van Wezel, T.; Uh, H. W.; Kenter, G. G.; Jan Fleuren, G. *Genes Chromosomes Cancer* **2009**, *48*, 410−418.

(3) Nam, R. K.; Zhang, W. W.; Trachtenberg, J.; Seth, A.; Klotz, L. H.; Stanimirovic, A.; Punnen, S.; Venkateswaran, V.; Toi, A.; Loblaw, D. A.; Sugar, L.; Siminovitch, K. A.; Narod, S. A. *Clin. Cancer Res.* **2009**.

(4) Khanna, M.; Park, P.; Zirvi, M.; Cao, W.; Picon, A.; Day, J.; Paty, P.; Barany, F. *Oncogene* **1999**, *18*, 27–38.

(5) Colomer, R.; Monzo, M.; Tusquets, I.; Rifa, J.; Baena, J. M.; Barnadas, A.; Calvo, L.; Carabantes, F.; Crespo, C.; Munoz, M.; Llombart, A.; Plazaola, A.; Artells, R.; Gilabert, M.; Lloveras, B.; Alba, E. *Clin. Cancer Res.* **2008**, *14*, 811–816.

(6) Fasching, P. A.; Kollmannsberger, B.; Strissel, P. L.; Niesler, B.; Engel, J.; Kreis, H.; Lux, M. P.; Weihbrecht, S.; Lausen, B.; Bani, M. R.; Beckmann, M. W.; Strick, R. *J. Cancer Res. Clin. Oncol.* **2008**, *134*, 1079–1086.

(7) Gusella, M.; Padrini, R. *Pharmacogenomics* **2007**, *8*, 985–996.

(8) Kim, S.; Misra, A. *Annu. Rev. Biomed. Eng.* **2007**, *9*, 289–320.

(9) Tost, J.; Gut, I. G. *Clin. Biochem.* **2005**, *38*, 335–350.

(10) Tang, K.; Fu, D. J.; Julien, D.; Braun, A.; Cantor, C. R.; Koster, H. *Proc. Natl. Acad. Sci. U.S.A.* **1999**, *96*, 10016–10020.

(11) Huh, Y. S.; Lowe, A. J.; Strickland, A. D.; Batt, C. A.; Erickson, D. *J. Am. Chem. Soc.* **2009**, *131*, 2208–2213.

(12) McCreery, R. L. *Raman Spectroscopy for Chemical Analysis*; John Wiley & Sons: New York, 2000.

(13) Lakowicz, J. R. *Principles of Fluorescence Spectroscopy*, 3rd ed.; Springer Science+Business Media, LLC: New York, 2006.

(14) Cao, Y. C.; Jin, R.; Mirkin, C. A. *Science* **2002**, *297*, 1536–1540.

(15) Mahajan, S.; Richardson, J.; Brown, T.; Bartlett, P. N. *J. Am. Chem. Soc.* **2008**, *130*, 15589–15601.

(16) Graham, D.; Mallinder, B. J.; Whitcombe, D.; Watson, N. D.; Smith, W. E. *Anal. Chem.* **2002**, *74*, 1069–1074.

(17) Jun, B. H.; Kim, J. H.; Park, H.; Kim, J. S.; Yu, K. N.; Lee, S. M.; Choi, H.; Kwak, S. Y.; Kim, Y. K.; Jeong, D. H.; Cho, M. H.; Lee, Y. S. *J. Comb. Chem.* **2007**, *9*, 237–244.

10.1021/ac100921b
Published on Web 06/08/2010

Table 1. Primers Used in LDR-SERS Experiments

template/primer	sequence for LDR (5′−3′)
common LDR primer	5Phos[a]/TGG CG/AmT[b]/AGG CAA GAG TGC CTT GAC
G12D mutant LDR primer	GAA TAT AAA CTT GTG GTA G/FlurT[c]/T GGA GCT G***A***
G12A mutant LDR primer	GAA TAT AAA CTT GTG GTA G/6FAM[d]/T GGA GCT G***C***
wild type LDR primer	GAA TAT AAA CTT GTG GTA G/TAM[e]/T GGA GCT G***G***

[a] 5Phos denotes a 5′ phosphorylation. [b] AmT denotes an aminated thymine. [c] FlurT denotes a fluorescein dT. [d] 6FAM denotes a 6-carboxyfluorescein dT. [e] TAM denotes a TAMRA dT. The 3′ base in mutant and wild type LDR primers (bold and italic) allow for specific discrimination of the two templates.

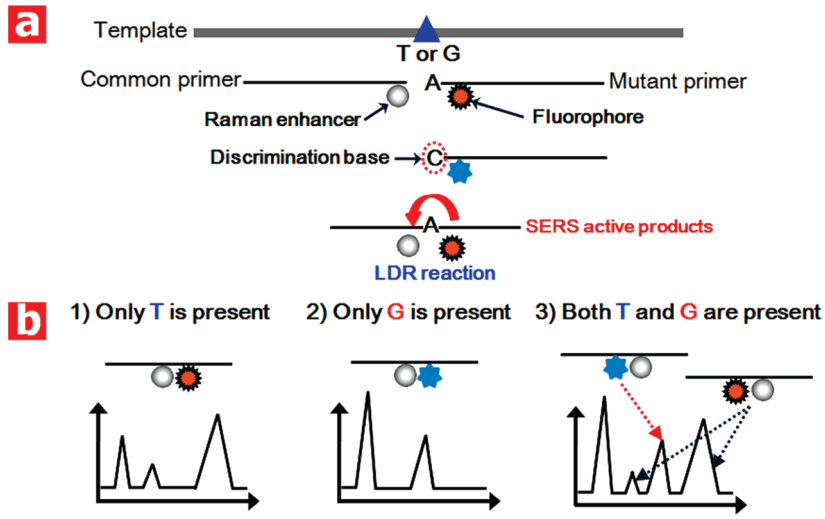

Figure 1. (a) Overview of LDR/SERS ligation and (b) schematic of multiplex SERS spectra. The silver spheres represent silver nanoparticles, and colored circles represent fluorophores.

Here we demonstrate the multiplex genotyping capacity of our LDR-SERS technology and how it may be used to identify multiple SNP alleles. Varying Raman enhancer and excitation wavelength conditions were tested to determine their effect on the signal-to-noise ratio of each peak cluster. Additionally, the direct correlation between diagnostic peak intensity and template concentration was demonstrated. Finally, a three-plex detection system was demonstrated with a 10 pmol limit of detection.

MATERIALS AND METHODS

Ligase Detection Reaction. Template DNA used in LDR reactions was genomic DNA extracted from nondiseased colon, DLD1, and SW1116 cell lines for WT, G12D, and G12A detection experiments, respectively. The oligonucleotide sequences of all the probes used in these experiments are shown in Table 1. All DNA primers were synthesized (Integrated DNA Technologies Coralville, IA) and adapted by previous work done by Khanna et al.[4] Thermostable 9° North DNA ligase and buffer were purchased from New England Biolabs (Beverly, MA). The LDR reaction contained the following in a 10 μL reaction: 20 pmol of template, 100 pmol of each primer, 1 μL of 9° N DNA ligase, 1 μL of supplied 9° N DNA ligase 10× buffer, and water to 10 μL. The LDR reactions used the following thermocycler program in a MJ Research PTC-200 Peltier Thermo Cycler: (1) 90 °C for 2 min, (2) 90 °C for 30 s, (3) 50 °C for 4 min, (4) repeat steps 2 and 3 29 times then 50 °C for 10 min, and (5) hold at 4 °C.

LDR Functionalization and Purification. The completed LDR reaction mixture was treated with 2 μL of DMSO, mixed, and allowed to sit for 2 min. A total of 100 pmol of the NHS ester of thioctic acid was added to the treated LDR reaction and allowed to react for 1 h. The reaction mixture was then added to 200 μL of 60 nm Ag or Au nanoparticles and allowed to react for 1 h and purified as previously described.[11]

Raman Spectroscopy Measurements. Raman measurements were made using an inVia Raman spectrometer (INVIA Medical Imaging Solutions, Ann Arbor, Michigan) coupled to a Leica microscope. The experiments were conducted by focusing the excitation laser on the electro-active microwell as previously described.[11,19] The 488 and 785 nm laser lines were used as optical excitation sources, and the scattered signal was collected by a Peltier-cooled CCD detector. A 50× (NA = 0.55) objective lens was used to focus the laser beam spot onto the sample surface with a diameter of about 2 μm. Wavenumbers ranging from 1100 to 1800 cm^{-1} were examined for all SERS experiments.

RESULTS AND DISCUSSION

An example of our multiplex LDR-SERS scheme is presented in Figure 1. An oligonucleotide primer, common to all haplotypes for a given gene locus, binds downstream of a SNP. This primer contains an amine for conjugation to a Raman enhancing nanoparticle after ligation has occurred. A second primer containing a Raman active fluorophore and a discriminating base at the 3′ end binds upstream of the SNP, adjacent to the first primer. This discriminating, terminal base allows for allele specificity, as ligation only occurs if the upstream primer matches perfectly with the

(18) Sun, L.; Yu, C.; Irudayaraj, J. *Anal. Chem.* **2008**, *80*, 3342–3349.

(19) Huh, Y. S.; Chung, A. J.; Cordovez, B.; Erickson, D. *Lab Chip* **2009**, *9*, 433–439.

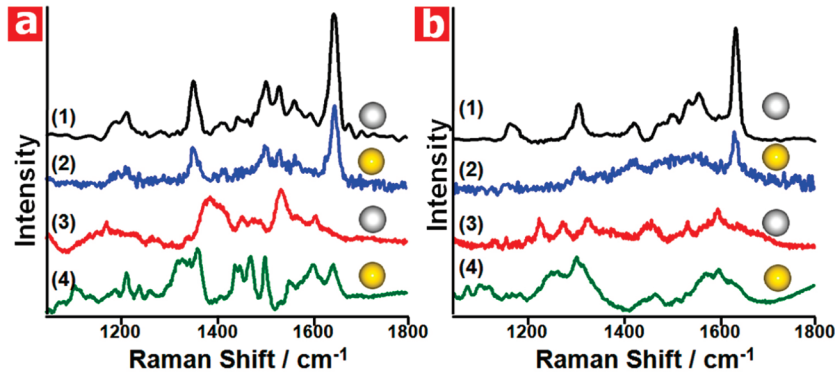

Figure 2. Investigation of Raman enhancers and excitation source. Samples 1 and 2 were excited at 488 nm while samples 3 and 4 were excited at 785 nm. Odd numbered samples contained silver Raman enhancers and even numbered samples contained gold Raman enhancers as indicated by colored spheres: (a) wild type TAMRA labeled DNA and (b) G12D mutant fluorescein labeled DNA.

DNA template. Therefore, the Raman signal will only be detected if ligation of the two primers occurs, since the Raman enhancer must be very close to the signal source. Different Raman active fluorophores are placed on the SNP allelic specific primers, which produce a signature Raman profile as diagramed in Figure 1b.

As described in Table 1, a TAMRA fluorescent label was attached to the wild type discriminating primer while a fluorescein and 6-carboxyfluorescein (6-FAM) labels were attached to the G12D and G12A discriminating primers, respectively. Samples containing all three templates produce an aggregate spectrum that has elements of all Raman reporters, but diagnostic peaks of each marker can still be discerned and quantified. After the ligation occurs, the Raman enhancer is attached to the DNA strand, purified, and then concentrated in an electroactive nanowell.[11,19]

Upon examination of the differences in spectra, several possible diagnostic peaks were identified with the most prominent at approximately 1315, 1370, and 1488 cm^{-1} for fluorescein (G12D), TAMRA (WT), and 6-FAM (G12A) labeled DNA, respectively. In order to optimize the SERS output signal and resolution between diagnostic peaks, the interplay between laser excitation wavelength and nanoparticle enhancers was investigated using a two-plex model. Figure 2a plots TAMRA labeled DNA SERS intensity as a function of laser excitation wavelength and Raman enhancers. While the 785 nm excitation source (Figure 2a(3),(4)) did provide 3-fold more intense peaks at the 1500 cm^{-1} cluster in the TAMRA sample, the 488 nm excitation source gave much more distinct peaks, reducing the peak width of the 1370 cm^{-1} diagnostic peak by a factor of 3 in both the silver and gold enhanced samples. A similar pattern was seen for fluorescein-labeled DNA in Figure 2b. The 488 nm laser provided an approximately 3-fold higher signal as compared to the 785 nm excitation source for the peak at 1650 cm^{-1} and a 1.4-fold average enhancement when comparing the silver enhanced samples. This is most likely attributable to a resonance Raman effect, where both dyes are excitable to their first electronic state at 488 nm but not at 785 nm.[16,20] Resonance Raman effects can greatly increase the Raman signal, which has been previously shown in assays detecting DNA base changes using the hybridization format.[14]

The difference between gold and silver nanoparticle SERS enhancers was also investigated, with silver nanoparticles providing a much better signal-to-noise ratio as seen in Figure 2. In the TAMRA labeled sample, silver provided an average 1.5 SNR enhancement over gold when averaging all the peaks and a 1.7-fold better SNR at the 1370 cm^{-1} diagnostic peak when excited at 488 nm. An average 1.33 SNR enhancement of silver compared to gold was achieved in the TAMRA sample excited at 785 nm. In the fluorescein labeled sample, an average 3.2 SNR was achieved over gold when excited at 488 nm. SNR of the fluorescein labeled samples excited at 785 nm was not readily comparable in silver versus gold enhancements due to the large peak broadness of the gold enhanced samples. The metal dependent, Raman enhancement trends conform to previously observed behavior that silver is often a better Raman enhancer than gold.[21] This effect is due to the localized surface plasmon resonance of the aggregated silver particles having a greater maximum absorbance than gold and better matching the excitation wavelength. Again, higher Raman signal output may be obtained by matching the excitation wavelength to the absorbance wavelength of the fluorescent label, inducing an electronic transition to achieve surface enhanced resonance Raman (SERRS). Quantitatively maximizing the Raman signal based on nanoparticle composition and excitation wavelength has been thoroughly analyzed previously.[22] Design and selection of Raman molecules for multiplex analysis have also been previously investigated.[23−25]

Figure 3 shows two-plex data obtained for a mixture of WT and G12D targets using both LDR primers. Figure 3a shows the SERS spectra profiles of a mixture of WT and G12D with silver or gold as the SERS enhancer (silver for 1 and 3, gold for 2 and 4) and an excitation wavelength of 488 nm (1 and 2) and 785 nm (3 and 4). The multiplex sample conformed to the trends observed in Figure 2, with silver nanoparticles demonstrating 1.5- and 2-fold SNR enhancement for the fluorescein and TAMRA diagnostic peaks, respectively, when excited at 488 nm as compared to gold. The 488 nm laser reduced the peak width of the fluorescein and TAMRA diagnostic peaks by a factor of 1.8 and 1.2, respectively, as compared to the 785 nm excitation source for silver enhanced

(20) Faulds, K.; McKenzie, F.; Smith, W. E.; Graham, D. *Angew. Chem., Int. Ed.* **2007**, *46*, 1829–1831.
(21) Zeman, E. J.; Schatz, G. C. *J. Phys. Chem.* **1987**, *91*, 634–643.
(22) Stokes, R. J.; Macaskill, A.; Lundahl, P. J.; Smith, W. E.; Faulds, K.; Graham, D. *Small* **2007**, *3*, 1593–1601.
(23) Faulds, K.; Smith, W. E.; Graham, D. *Anal. Chem.* **2004**, *76*, 412–417.
(24) Graham, D.; Faulds, K. *Chem. Soc. Rev.* **2008**, *37*, 1042–1051.
(25) Graham, D.; Faulds, K.; Thompson, D.; Mackenzie, F.; Stokes, R.; Macaskill, A. *Biochem. Soc. Trans.* **2009**, *37*, 441–444.

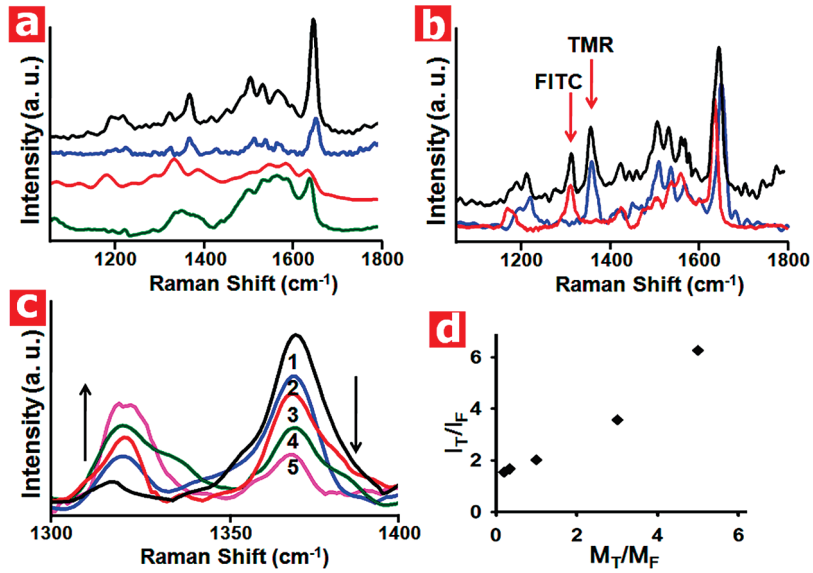

Figure 3. Two-plex SNP samples: (a) mixed genotype SERS spectra. (b) Overlay of singleplex SERS spectra with WT in blue and G12D mutant in red against the multiplex spectrum in black. TAMRA and fluorescein diagnostic peaks are highlighted with labeled arrows. (c) Diagnostic peak intensities of mix genotype samples, varying the LDR template concentration of mutant to wild type template DNA as (1) 0.1:1, (2) 0.5:1, (3) 1:1, (4) 3:1, (5) 5:1. (d) Plot of template molar ratio against diagnostic peak intensity. *I* denotes intensity, *M* denotes moles, T denotes TAMRA, and F denotes fluorescein.

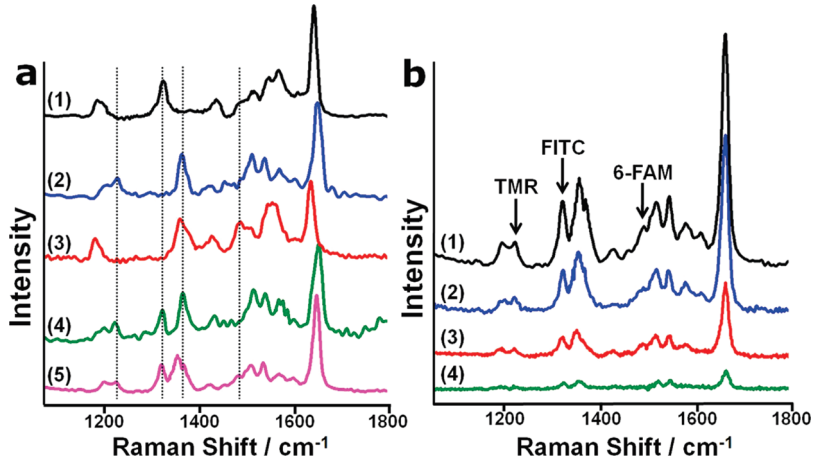

Figure 4. Multiplex SNP samples: (a) (1) G12D (fluorescein) mutant, (2) WT KRAS (TAMRA), (3) G12A (6-FAM) mutant, (4) WT & G12D 2-plex, (5) WT, G12D, G12A 3-plex. Dotted lines indicate diagnostic peaks. (b) Dilution series of LDR three-plex containing variable amounts of template: (1) 20, (2) 10, (3) 5, and (4) 2 pmol.

samples. Figure 3b shows a resultant two-plex spectra with the fluorescein and TAMRA spectra overlaid, demonstrating that the diagnostic fluorescein peak at ~1315 cm^{-1} is clearly distinguishable from the diagnostic TAMRA peak at ~1370 cm^{-1}, which identify the G12D mutant and wild type genotypes, respectively. These spectra were obtained from silver enhanced samples excited at 488 nm. Figure 3c depicts the correlation of SNP concentration to signal intensity. In the mixed sample, the population of the mutant (fluorescein) to wild type (TAMRA) DNA template was varied in the LDR reaction of at ratios of 0.1:1, 0.5:1, 1:1, 3:1, and 5:1 in samples 1−5, respectively. As expected, as the ratio of mutant to WT SNPs is increased, the 1315 cm^{-1} signal increases while the 1370 cm^{-1} signal decreases.

Figure 3d plots the molar ratio of WT to mutant template concentration against signal intensity of the diagnostic peaks as obtained from Figure 3c. A linear trend is generated with diagnostic signal intensity directly correlating to the genotype molar ratio. Unlike PCR, LDR does not produce exponential amplification of the product since the product of the ligation is not a template for the LDR primers. The signal is linear with the initial target concentration.

Figure 4 demonstrates three-plex capabilities of the system. In the presence of all three diagnostic primers, LDR reactions were run with one, two, or three templates then functionalized with silver nanoparticles and their Raman spectra analyzed. Figure 4a(1) shows a diagnostic peak for the G12D mutant (fluorescein) at approximately 1315 cm^{-1}. Parts a(2) and a(3) pf Figure 4 are representative spectra for WT (TAMRA) and G12A (6-FAM) haplotypes, respectively. While 1370 cm^{-1} was potentially a diagnostic peak for TAMRA-labeled WT templates, it overlaps with the 6-FAM peak seen for the G12A allele. An alternative diagnostic peak for the WT spectrum can be seen at ~1225 cm^{-1}, however, and can be used for WT haplotype identification. The G12A haplotype has a unique diagnostic peak at

$\sim$1488 cm^{-1}. Figure 4a(4) demonstrates that the presence of all three diagnostic primers in the reaction not inhibit two-plex detection, as diagnostic peaks for WT and G12D mutations are present. Figure 4a(5) demonstrates detection of all three haplotypes with diagnostic peaks for all three alleles clearly present. Figure 4b shows a dilution series that demonstrates a 10 pmol limit of detection.

CONCLUSIONS

Here we have demonstrated an important step toward a LDR-SERS detection platform for SNPs. This system allows accurate discrimination of multiple alleles and does not require a microarray format or capillary electrophoresis.[26] Additionally, it displays the ability to quantify SNP allelic ratios based on relative signal intensity. This technology is an important advancement in moderate scale SNP detection as it retains the advantages previously shown with LDR and increases the potential for multiplex detection in a relatively simple technology platform. SERS multiplex detection of oligonucleotides labeled with common fluorophore tags has been previously demonstrated.[27,28] It is important to note that fluorophores are often used as Raman tags due to their wide availability on oligonucleotides, but any chromophore or molecule with a high Raman cross section and unique spectral signature could be used as a label.[29,30] This opens up a very large spectral space for detection and multiplexing possibilities. Multiplexing is particularly amenable to this system because even if diagnostic peaks overlap, their sources can still be determined through spectral fitting analysis, which identifies peaks not discovered by linear analysis and direct observations.[28] Furthermore, isotopically different variants of a given probe may be detected as different signals allowing for further multiplexing.[31] Because of the adaptability and sensitivity of our system, we believe our technology is a step toward an eventual point-of-care genotype analysis system for clinically relevant SNPs. In order to achieve this point-of-care goal, attachment of Raman enhancers to oligonucleotides prior to the ligase detection reaction must be achieved and is currently being investigated.

ACKNOWLEDGMENT

This work was supported in part by the National Institute of Justice (NIJ Grant No. 2004-DN-BX-K001 to C.A.B.), the Cornell Nanobiotechnology Center Integrated Research Fund, and the Ludwig Institute for Cancer Research. The authors of this manuscript claim no competing financial interests.

Received for review April 8, 2010. Accepted May 31, 2010.

AC100921B

(26) Tobler, A. R.; Short, S.; Andersen, M. R.; Paner, T. M.; Briggs, J. C.; Lambert, S. M.; Wu, P. P.; Wang, Y.; Spoonde, A. Y.; Koehler, R. T.; Peyret, N.; Chen, C.; Broomer, A. J.; Ridzon, D. A.; Zhou, H.; Hoo, B. S.; Hayashibara, K. C.; Leong, L. N.; Ma, C. N.; Rosenblum, B. B.; Day, J. P.; Ziegle, J. S.; De La Vega, F. M.; Rhodes, M. D.; Hennessy, K. M.; Wenz, H. M. *J. Biomol. Technol.* **2005**, *16*, 398–406.

(27) Faulds, K.; Jarvis, R.; Smith, W. E.; Graham, D.; Goodacre, R. *Analyst* **2008**, *133*, 1505–1512.

(28) Lutz, B. R.; Dentinger, C. E.; Nguyen, L. N.; Sun, L.; Zhang, J.; Allen, A. N.; Chan, S.; Knudsen, B. S. *ACS Nano* **2008**, *2*, 2306–2314.

(29) Fruk, L.; Grondin, A.; Smith, W. E.; Graham, D. *Chem. Commun.* **2002**, 2100–2101.

(30) Sun, L.; Yu, C.; Irudayaraj, J. *Anal. Chem.* **2007**, *79*, 3981–3988.

(31) Perera, P. N.; DebS. K.; Davisson, V. J.; Ben-Amotz, D. *J. Raman Spectrosc.* DOI: 10.1002/jrs.2513.